http://dx.doi.org/10.1016/j.jmb.2012.07.026 J. Mol. Biol. (2012) 423, 462–471

Contents lists available at www.sciencedirect.com

Journal of Molecular Biology

journal homepage: http://ees.elsevier.com.jmb

From a Ratchet Mechanism to Random Fluctuations Evolution of Hsp90's Mechanochemical Cycle

Christoph Ratzke[1], Minh N. T. Nguyen[2], Matthias P. Mayer[2] and Thorsten Hugel[1,3*]

[1]*Physik-Department (E22a), Institute of Medical Engineering, Technische Universität München, 85748 Garching, Germany*
[2]*Zentrum für Molekulare Biologie der Universität Heidelberg (ZMBH), DKFZ-ZMBH-Alliance, 69120 Heidelberg, Germany*
[3]*Center for NanoScience, Center for Integrated Protein Science Munich, Technische Universität München, 85748 Garching, Germany*

Received 3 March 2012;
received in revised form
5 July 2012;
accepted 31 July 2012
Available online
6 August 2012

Edited by R. L. Gonzalez

Keywords:
chaperone;
FRET;
Hsp90;
HtpG;
single molecule

The 90-kDa heat shock proteins [heat shock protein 90 (Hsp90)] are a highly conserved ATP-dependent protein family, which can be found from prokaryotic to eukaryotic organisms. In general, Hsp90s are elongated dimers with N- and C-terminal dimerization sites. In a series of publications, we have recently shown that no successive mechanochemical cycle exists for yeast Hsp90 (yHsp90) in the absence of clients or cochaperones. Here, we resolve the mechanochemical cycle of the bacterial homologue HtpG by means of two- and three-color single-molecule FRET (*F*örster *r*esonance *e*nergy *t*ransfer). Unlike yHsp90, the N-terminal dynamics of HtpG is strongly influenced by nucleotide binding and turnover—its reaction cycle is driven by a mechanical ratchet mechanism. However, the C-terminal dimerization site is mainly closed and not influenced by nucleotides. The direct comparison of both proteins shows that the Hsp90 machinery has developed to a more flexible and less nucleotide-controlled system during evolution.

Introduction

In virtually all living organisms from time to time, cells experience elevated temperatures or other stresses such as mechanical stress, water deprivation, noxious compounds, infection, or inflammation. The necessity to protect cells from such stresses led to the development of a class of proteins called heat shock proteins.[1] One of these proteins is the heat shock protein 90 (Hsp90) (reviewed in Refs. 2–5), which is structurally highly conserved over a large variety of organisms but seems to have evolved significant differences in respect to their molecular mechanism and functionality.[6] In many eukaryotes, Hsp90 is essential in unstressed cells; thus, a knockout of Hsp90 is lethal for eukaryotic organisms, while it is not lethal for prokaryotes. Up to now, cochaperones of Hsp90 are only known in eukaryotic systems.

Hsp90s are homodimers, each protomer consisting of three domains: an N-terminal nucleotide binding domain, a middle domain, and a C-terminal dimerization domain. Several of these domains undergo large conformational changes with respect to each other. The N-terminal conformational changes of the eukaryotic yeast Hsp90 (yHsp90) have recently been investigated. Although closing of

*Corresponding author. Physik-Department (E22a), Institute of Medical Engineering, Technische Universität München, 85748 Garching, Germany. E-mail address: thugel@mytum.de.

Abbreviations used: Hsp90, heat shock protein 90; yHsp90, yeast Hsp90; 2D, two-dimensional.

0022-2836/$ - see front matter © 2012 Published by Elsevier Ltd.

the N-terminal domains was observed in the presence of the unnatural nucleotide AMP-PNP, natural nucleotides do not cause measurable closing of the dimers.[7] Moreover, the N-terminal conformational changes of yHsp90 are hardly coupled to the turnover of nucleotides.[8] Therefore, no successive reaction cycle exists for yHsp90, but this protein is thermally driven through a network of states (including C-terminal open and closed states).[9]

In contrast, studies on HtpG (the bacterial homologue of yHsp90) show that ATP is strongly coupled to large conformational changes.[10–12] To investigate the details of the conformational dynamics of HtpG and its nucleotide dependence, we used a three-color single-molecule FRET (*F*örster *r*esonance *e*nergy *t*ransfer) setup similar to the studies on yHsp90. We could indeed observe large conformational changes in several domains of HtpG upon ATP turnover. Most interestingly, ATP fixes a closed state that was previously reached by thermal fluctuations—such a mechanism is called a *mechanical ratchet* (for an exact definition, see Supplementary Text and Supplementary Fig. 10). However, the C-terminal domains of HtpG are closed most of the time without being affected by nucleotide binding. Therefore, we find a large difference in the mechanisms of yHsp90 and HtpG, although they are structurally homologous. This sheds a new light onto the evolution of the Hsp90 family, which obviously went from the quite strictly nucleotide-regulated HtpG to the randomly fluctuating yHsp90, whose conformation is only weakly affected by nucleotides.

Results

Nucleotides regulate the large N-terminal conformational changes of HtpG

To investigate the conformational dynamics and the nucleotide dependence of HtpG, we used the single-molecule assay previously described for yHsp90.[8,9] Different HtpG cysteine mutants, which have cysteines in either the N-domain (61C) or the middle domain (341C) or two cysteines within one monomer (61C and 341C), have been used (Fig. 1, left); these positions are homologous to the positions 61 and 385 used in yHsp90. All the mutants had a coiled-coil motif added to their C-terminus to keep the two monomers in close proximity as described previously[8,13] and show wild-type ATPase activity (Supplementary Table 1). The mutants with cysteine in different monomers were simultaneously labeled with Atto550 and Atto647N dyes and then biotinylated. The mutant with two cysteines in one monomer was also simultaneously labeled with these two dyes, and then, the labeled monomers were exchanged with biotinylated HtpG to get heterodimers (for detailed protocols, see Supplementary Information). This results in heterodimers with one biotinylated and the other labeled with two dyes. Homodimers of dye-labeled monomers did not attach to the substrate while homodimers of biotinylated monomers gave no fluorescence signal.

Excitation of the donor dye (Atto550) leads to a distance-dependent energy transfer to the acceptor dye (Atto647N). From the intensities of the two dyes, the FRET efficiency was calculated as described previously.[8] This FRET efficiency is linked to the distance between the dyes and therefore to the conformational state. Incomplete labeling did not disturb the measurement because proteins that carried no dye or the same dye twice showed no FRET signal at all and were therefore ignored. This allowed the real-time observation of the movement of the N-terminal and middle domains, as well as the movement within a single monomer of Hsp90. Characteristic FRET efficiency curves are shown in Fig. 1 (right). All the obtained FRET efficiencies for one experimental condition were collected and plotted in histograms as shown in Fig. 2. In those plots, the different occurring conformational species can be distinguished since the FRET signal is not averaged as in bulk measurements. All histograms in Fig. 2 have their main peaks at FRET efficiencies higher than 0.5, which means that HtpG stays mainly in a compact, closed state. This is a clear contrast to yHsp90, which stays more in the open state under natural nucleotide conditions.[8]

In the absence of nucleotide, the N-terminal domain is more or less continuously moving (Fig. 1a, the typical slight upward trend is discussed later), without staying in the open or closed state. This leads to values over the whole range in the corresponding FRET histogram (Fig. 2a). In contrast, the middle domains are mainly closed with rare opening events (Fig. 2b). The movement between the N-terminal domain and the middle domain within a monomer in the absence of nucleotides (Fig. 2c) is less pronounced; it is mainly fixed with no large movement of the domains relative to each other. Nevertheless, it becomes even less flexible upon the addition of ATP (Fig. 2f) or ADP (Fig. 2i), which both have smaller peak widths compared to Fig. 2c. Altogether, in the absence of nucleotide, the N-domain shows large conformational fluctuations, whereas the middle domain stays mainly in a closed state.

In the presence of 2 mM ATP, the situation changes considerably; in essence, the N-domain and the M-domain are now permanently closed (Figs. 1b and 2d) and the monomer chains become very rigid. This can be seen by a single sharp high FRET peak for the N–N domain distance (Fig. 2d), as well as for the N–M intra-monomer distance (Fig. 2f). Surprisingly, the middle domain shows a few opening events, which can be seen on the "tail"

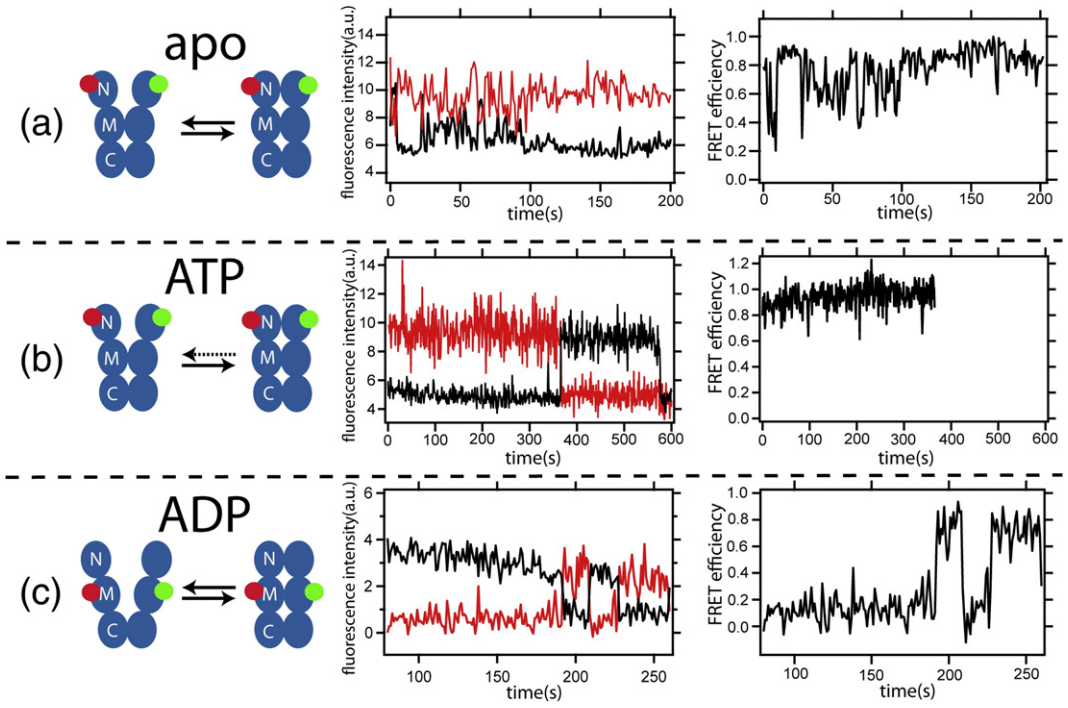

Fig. 1. Schematics of HtpG constructs and FRET example traces. The left side shows the position of the dyes and the conformational transitions investigated. In the middle column, the fluorescence raw data are shown (red, acceptor; black, donor), and on the right side, the obtained FRET efficiencies are depicted. (a) Without nucleotide, the N-terminal domain is wobbly without showing discrete state transitions. (b) With ATP, the N-terminal domain stays mainly in the closed state (here, for about 365 s until the dye bleaches). FRET efficiencies after bleaching are not evaluated and therefore not shown. (c) With ADP, the M-domain shows quite slow transitions between a discrete open state and a closed state. See Fig. 2 for a full account of all combinations of nucleotide conditions and domains.

of lower FRET efficiencies in Fig. 2e (for an example curve, see Supplementary Fig. 1). Thus, a rare "O-like" form of HtpG exists in the presence of ATP. Altogether, ATP leads to a mainly closed conformation, with occasional flexibility in the middle domain.

In the presence of 2 mM ADP, again, conformational dynamics can be observed. In contrast to the situation without nucleotide, well-defined conformational states can be found—mainly, one open state and one closed state. Rarely, a third state with a FRET efficiency of around 0.5 can be observed (an example curve is shown in Supplementary Fig. 2). Furthermore, conformational transitions between the two major populated states occur (Fig. 1c). These transitions are very slow for proteins: the dwell times are around 25 s and even more (see Supplementary Information for details). Thus, only a very small amount of dwell times could be extracted, and we have to restrict ourselves to a qualitative discussion of the kinetics in the presence of ADP. The energy barrier that separates those states has to be much larger than the thermal energy. In contrast to the situation in the absence of nucleotide, the conformational changes are not limited to the N-terminal domain, but the N- and M-domain movements seem to be correlated. This can be seen by the fact that the FRET histograms for both domains (Fig. 2g and h) show two states approximately equally distributed, and also, the obtained FRET time traces for both processes show long dwell times (Fig. 1c and Supplementary Fig. 3).

These data allow a reaction cycle for HtpG to be formulated. In the nucleotide-free state, the M-domain is mainly closed while thermally driven random movement of the N-domain occurs as there is no other energy source. After addition of ATP, HtpG is fixed into an overall closed and rigid state. In the presence of ADP (i.e., after hydrolysis), HtpG can slowly switch between defined open and closed states.

In addition, of that, the FRET histograms allow the estimation of the distances between the dyes. These values should only be taken as estimates since several factors impact the exact conversion from FRET efficiencies to distances.[14] Free rotation of the dyes was confirmed by fluorescence anisotropy measurements (Supplementary Table 4). Nevertheless, relative distance changes are generally reliable and distances determined by FRET have been self-consistent and in good agreement with crystal structures in the past.[8,9,15] The obtained distances for HtpG are given in Supplementary Table 2. The distance between the dyes at the N-termini in the

closed state is 4.9 nm without nucleotide and in the presence of ADP, whereas after ATP binding, it is around 4.3 nm and thus more compact. Without nucleotides, the FRET efficiency values fall to around 0.2 corresponding to a distance of 8 nm. An extremely extended structure as described recently[16] would result in zero FRET efficiency. If at all, such a widely open structure only rarely exists (Fig. 2a shows a few data points around zero FRET efficiency) and can therefore be neglected in the following. The closed state of the middle domain shows a distance of approximately 5.5 nm between the cysteines at position 341, while the cysteines at the C-terminal position 521 are separated by about 5.2 nm.

HtpG is driven by a mechanical ratchet mechanism

How does ATP binding and hydrolysis drive these conformational changes? In general, there are two major possibilities, either ATP binds to the open state of HtpG and forces it into the closed state or HtpG moves into the closed state by thermal fluctuation where ATP binds and fixes HtpG there. The first model is often referred to as power stroke; the second, as mechanical ratchet (see Supplementary Fig. 10 for details).

In order to gain more information about the underlying mechanisms of HtpG, we performed three-color FRET measurements with 1 μM labeled ATP, similar to those performed recently for yHsp90.[15] Such high concentrations of labeled ATP are necessary because the dissociation constant for ATP is higher for HtpG compared to yHsp90 and they became possible by further improving the three-color FRET setup utilized for our yHsp90 studies. The HtpG was labeled at position 61 with Atto488 on one monomer and with Atto550 on the other monomer. The ATP was labeled at the γ position via a C-6 linker with Atto647N. The labeled ATP is hydrolyzed by HtpG 61C with wild-type activity (Supplementary Fig. 4). A schematic representation can be seen in Fig. 3c (right). These measurements simultaneously show the conformational and nucleotide binding dynamics of HtpG. Furthermore, they permit the direct detection of the

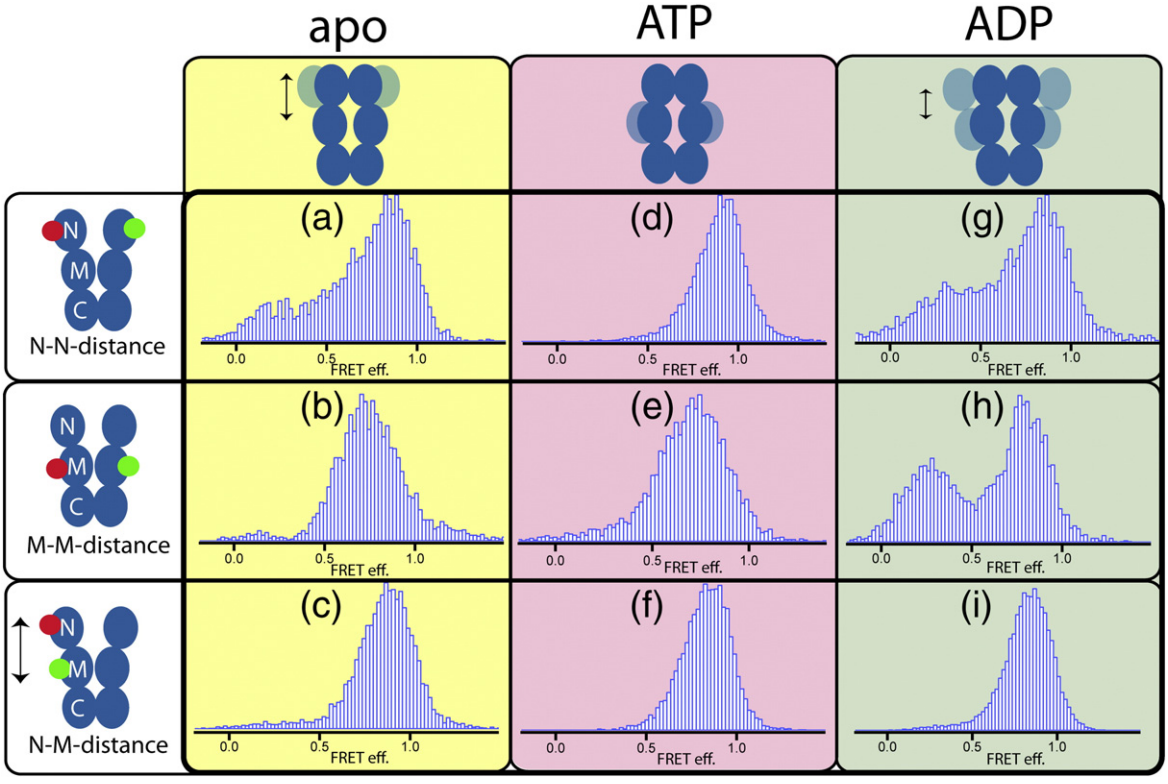

Fig. 2. Conformational changes of HtpG domains upon addition of nucleotides. Histograms of the FRET efficiencies for the various constructs and nucleotide conditions are depicted. The *y*-axes show relative numbers (normalized to an integral of 1), and the *x*-axes show the FRET efficiencies. (a–c) Without nucleotide, the N-domain is very flexible showing no discrete state transitions, whereas the middle domains are mainly closed. (d–f) With ATP, both dimers are quite close together and the monomers are very stiff, whereas with ADP (g–i), two clear states (one open and one closed) exist. The schemes on the upper row show the underlying conformational states. Dark blue is highly occupied and light blue is rarely occupied. The number of data points in each graph ranges from more than 4000 (N=32 molecules) (a) to almost 17,000 (N=98 molecules) (i).

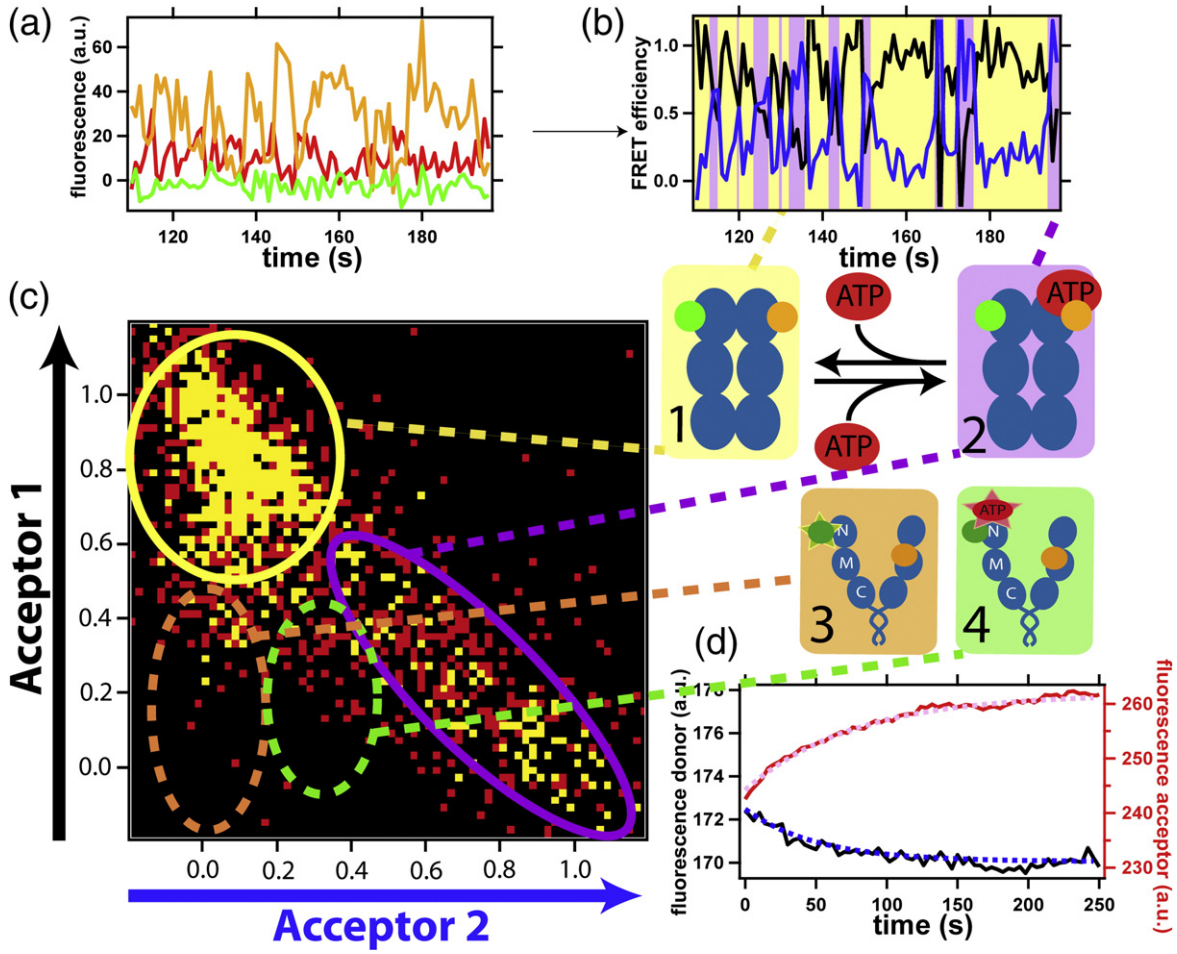

Fig. 3. Coordination between ATP binding and the open–close kinetics of HtpG. (a) Fluorescence signal *versus* time for a three-color FRET curve (green is Atto488 attached to one HtpG monomer at position 61C, orange is Atto550 attached to the other HtpG monomer at position 61C, and red is Atto647N attached to the ATP). The three fluorescence signals are converted into two partial fluorescence signals (b) by dividing the acceptor 1 (black) and the acceptor 2 (blue) signals by the total signal. Two types of binding curves can be observed, a fast binding and release dynamics (b) and a quite stable binding of ATP (Supplementary Fig. 7). The partial fluorescence intensities are plotted in 2D histograms (c) where the closed state without (1, yellow) and with (2, magenta) ATP bound can be separated (red square is one data point, and yellow is two or more data points for that pixel; the overall number of data points is 2000 from $N=20$ molecules). The green/brown broken circles indicate where the open state with/without ATP would occur (see Ref. 15 and Supplementary Fig. 9). The boxes with the Hsp90 schematics show the different possible states. The underlying colors also mark the position of every state in the 2D histogram (d) and in the example curve (b). (d) Bulk measurements of fluorescently labeled ATP (acceptor, red trace) binding to HtpG (donor, black trace). The broken lines are a global fit of the data with a time constant of 70±27 s (the error was estimated from three independent measurements). This slow binding process occurs because HtpG has to move into the N-terminal closed state before ATP can bind.

coupling between both processes and, therefore, give the causal order of reaction steps. From the three fluorescence intensities (Fig. 3a), two partial efficiencies are obtained (see Supplementary Text), which are best represented in two-dimensional (2D) FRET histograms (Fig. 3c).[17,18] The fluorescence traces are selected by a threshold criterion in the Atto647N detection channel (which reflects ATP binding) and subsequent manual inspection.

The first finding is that the fraction of HtpG dimers showing ATP binding is less than one-tenth of the fraction observed for yHsp90, which already suggests that not all conformational states are binding competent. Indeed, only single-molecule traces similar to the example in Fig. 3a and b could be obtained. The high acceptor 1 signal (black) in between the binding events in Fig. 3b clearly shows that ATP binding (high acceptor 2 signal; blue) takes place only in the closed state. These curves result in two peaks in the 2D histograms for the closed state without (yellow) and with (magenta) ATP (Fig. 3c). The position and shape of the peaks is equal to those

obtained for yHsp90 (see Ref. 15 and Supplementary Fig. 9). Binding of ATP in the open state was never observed in the more than 5000 observed molecules.

The open states would occur at the bottom left of the 2D histogram. In the case of yHsp90, the open apostate was within the orange broken circle and the open ATP-bound state was in the green broken circle (Ref. 15 and Supplementary Fig. 9). There is no significant number of data points for HtpG. Therefore, HtpG binds ATP only in the N-terminally closed state and has to convert into the closed binding-competent state before ATP binding can take place. We cannot exclude occasional binding of ATP to the open state at very high ATP concentration, but this is irrelevant for the mechanochemical cycle, as the affinity is at least 3 orders of magnitude lower and therefore negligible compared to the binding in the N-terminal closed state. Our data eliminate models where ATP bound to the N-terminal open state forces HtpG into the closed state (see Discussion for more details). Thus, the large conformational changes of HtpG are caused by a ratchet mechanism not by a power stroke.

Figure 3d shows bulk measurements of the ATP binding with 1 μM labeled HtpG and 10 μM labeled ATP. The obtained curve shows an effective binding rate, around 1/70 s. To exclude artifacts caused by fluorophore physics, we repeated the measurements with unlabeled HtpG and labeled ATP, as well as with labeled HtpG and unlabeled ATP (same concentrations as above). Neither of the control led to any signal change (Supplementary Fig. 5). The effective binding rate (~1/70 s) is far slower than ATP binding to the closed state itself (few seconds) as can be seen in Fig. 3a and b. Thus, as predicted by our ratchet mechanism and discussed in detail below, ATP binding is limited by the transition into the closed binding-competent state (with a rate of ~1/70 s).

The C-terminal dimerization site is not influenced by nucleotides

In the case of yHsp90, we recently described a C-terminal opening and closing on the timescale of seconds in addition to the N-terminal conformational changes. The opened–closed equilibrium was regulated by nucleotide binding at the N-terminus, demonstrating an N- to C-terminal communication in yHsp90.[9] To check if similar effects can be found in HtpG, we used an HtpG mutant without a zipper and with a cysteine in the C-terminal domain (521C), which also showed wild-type ATPase rate (Supplementary Table 1). The HtpG mutant was labeled and encapsulated in lipid vesicles as described previously for yHsp90.[9]

Figure 4a shows the FRET histograms for the C-terminal domain under various nucleotide conditions. The C-terminus is not affected by nucleotides, staying mainly in the closed state and only rarely can it be found in the open state (some values can be seen at lower FRET efficiencies in Fig. 4). This is in contrast to the situation in yHsp90 where rich C-terminal dynamics on the timescale of seconds was found. Moreover, in yHsp90, we found that the N- and C-terminal dynamics are anti-correlated, resulting in slow monomer exchange, with a time constant of around 1000 s, despite opening rates at the N-terminus and the C-terminus in the range of a few seconds. To test if similar effects can be found for HtpG, we performed monomer exchange experiments by mixing two differently labeled HtpG

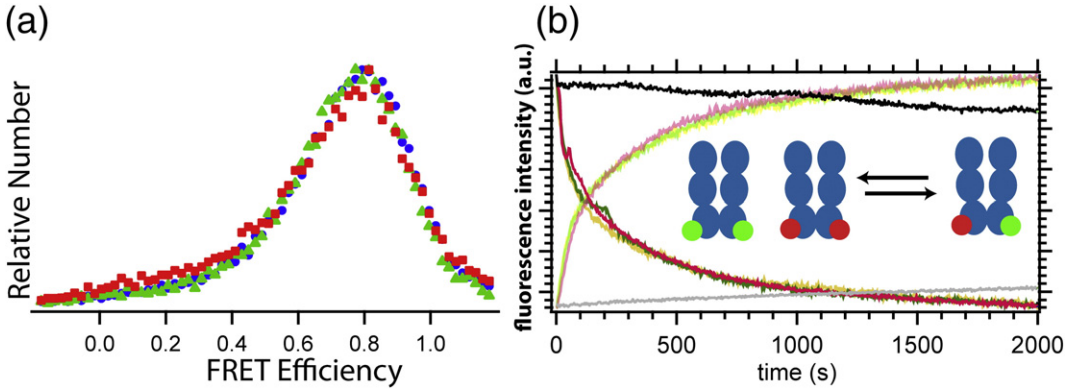

Fig. 4. Stability of the C-terminal dimerization for HtpG. (a) Single-molecule data show that the C-terminal domain is mainly closed (high FRET efficiency around 0.8) with rare opening events (few events at low FRET efficiency close to 0). No significant effect of nucleotides can be seen. Blue circles, ADP (total of 22,000 data points); red squares, ATP (total of 13,000 data points); green triangles, no nucleotide (total of 10,000 data points). (b) Bulk measurements show no effect of natural nucleotides on monomer exchange (dark curves are donor signal and bright curves are acceptor signal; yellow is without nucleotide, red is with 2 mM ADP, and green is with 2 mM ATP). Therefore, the N-terminal conformation is not relevant for C-terminal dimerization stability. Only the unnatural nucleotide AMP-PNP (2 mM) leads to a significant slowdown of the exchange rate (black).

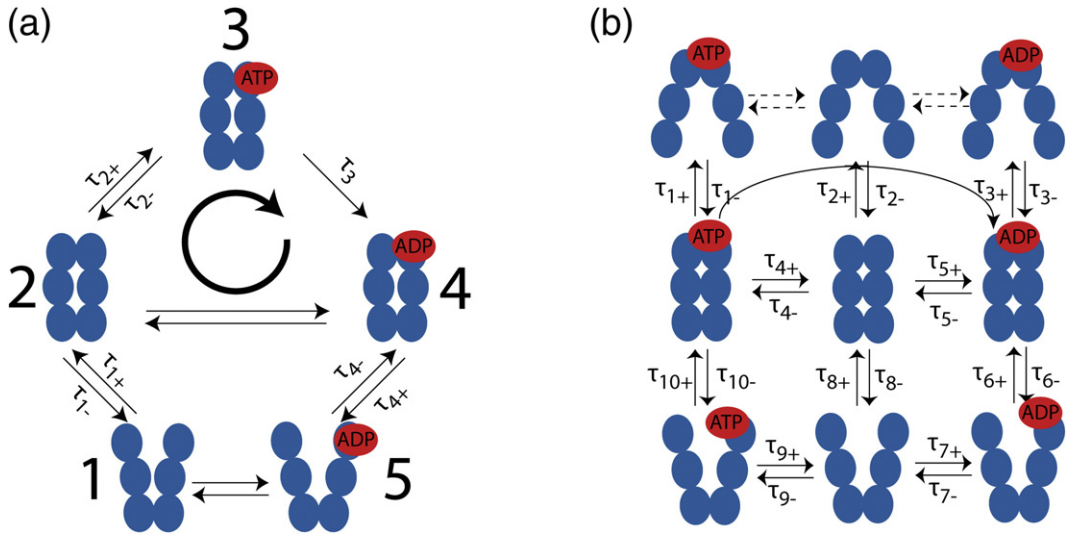

Fig. 5. Comparison and evolution of HtpG and yHsp90 reaction cycles. (a) ATP causes the closure of HtpG by a mechanical ratchet mechanism. ATP binds after N-domain closure and fixes this state (2→3). Thus, the system proceeds in ordinal succession through the states 2, 3, and 4. The C-terminal domains are mainly closed. (b) In contrast for yHsp90, no successive reaction cycle exists. The protein diffuses in random order through a network of states including N- and C-terminal opening and closing. The underlying energy landscapes are shown in Supplementary Fig. 8 and the rates are given in Supplementary Table 3.

species and measured the FRET signal upon formation of heterodimers (Fig. 4b), as described previously.[9] For HtpG, the effective mean exchange time is around 150 s (for details, see Supplementary Text) and thus faster than in the case of yHsp90, although the C-terminal dimerization is stronger. We repeated the measurement with 10× lower concentration to exclude that the measurement is diffusion limited and indeed found the same result (Supplementary Fig. 6). Only the nonnatural nucleotide AMP-PNP led to a strong slowdown of the exchange rate.

In summary, in contrast to yHsp90, no effect of natural nucleotides could be found on the exchange process or the C-terminal dynamics. Furthermore, the N-terminal dimerization state, which is changed by nucleotides, does not influence the exchange rate, which means that even complete N-terminal closing as in the presence of ATP does not alter the exchange rate. Thus, no N–C communication of the type found in yHsp90 exists in HtpG.

Discussion

In this work, we dissected the mechanochemical cycle of HtpG, the bacterial homologue of yHsp90. Most interestingly, the turnover of ATP causes large conformational changes of the N-terminal domain in HtpG, while the N-terminal conformational changes are only weakly coupled to ATP turnover in yHsp90. As discussed in the following, HtpG is driven by a ratchet mechanism, while yHsp90 is dominated by thermal fluctuations, which sheds a new light on the evolution of this important heat shock protein.

Figures 1 and 2 show that HtpG occupies many states and is very flexible in the N-domain without nucleotide and becomes rigidly closed upon binding of ATP. In the presence of ADP, a slow thermally driven transition between well-defined opened and closed states can be found. These results are consistent with HD (*h*ydrogen–*d*euterium) exchange data, where high flexibility was observed in the nucleotide-free state while significant stabilization was observed in the presence of ATP, especially in the N-domain.[11]

The kinetics of the HtpG mechanochemical cycle was further dissected with our three-color FRET experiments (Fig. 3). A schematics of this cycle is depicted in Fig. 5a. The apo-HtpG (no nucleotide) has to reach the closed state via thermal fluctuations (1↔2) in order to be able to bind ATP (2↔3) with high affinity. At physiological ATP concentrations, binding of ATP (2→3) is then much faster than the N-terminal opening (2→1) and HtpG therefore stays mainly in the closed state. Some of the ATP is then fixed and committed for hydrolysis (3→4). This step is rate limiting for the steady-state ATPase, and the similarity of the timescales between the ATPase and the closing is coincidental. The amount of committed ATP was determined to be around 15% from HD exchange data.[11] Such a committed state would require the occasional transition from weakly bound ATP to strongly bound ATP, which then awaits slow hydrolysis—indeed, we observe the occasional long binding of ATP in our FRET assay (e.g., see Supplementary Fig. 7). Finally, HtpG

is left in the ADP-bound state (4↔5), where the N-domain and the M-domain move together and thus a kind of hinge exists between the C-domain and the M-domain. Indeed, an increase in flexibility upon ADP binding could also be found by HD exchange.[11] In summary, the system proceeds in an ordinal cycle through the states 2, 3, and 4. Here, the rate constants can only be given as rough estimates since either no discrete transitions (apostate) or too few transitions (ADP state, ATP binding) could be observed for a quantitative analytics. Nevertheless, at least the order of magnitude of the temporal transitions can be given here.

ATP binding in the open state with subsequent fast closure, altogether taking less than 100 ms (the time resolution of our setup), can also be excluded. In this case, we would observe single-molecule traces where a closed state with bound ATP follows an ATP-free open state, which we never observed. Finally, we can exclude that HtpG opens after ADP release, binds ATP, and is closed by a power stroke, all within less than 100 ms. In this case, bulk experiments would show an immediate (<100 ms) transition to the closed state after addition of ATP, but it was shown that this process takes around 1 min.[11]

This cycle is in strong contrast to the situation in yHsp90, where nucleotides can bind in either the open or the closed state without directing large conformational changes.[15] Thus, yHsp90 does not show an ordinal reaction cycle, but the protein mainly diffuses through a network of states in random order (Fig. 5b). Another striking difference between HtpG and yHsp90 can be found in the different properties concerning the C-terminal domain. In HtpG, the C-terminal domain is mainly closed and unaffected by nucleotide binding at the N-terminus, whereas in yHsp90, C-terminal dynamics that is influenced by nucleotide binding was found. Such dynamics require N–C communication in yHsp90 causing anti-correlated N- and C-terminal movements. Consequently, yHsp90 dissociates slowly ($\tau \approx 1000$ s) despite the fact that N- and C-terminal ends open frequently. HtpG dissociates considerably faster, even in the ATP-bound (N-terminal closed) state. This suggests that the N-termini are not entangled in the natural cycle. Only with AMP-PNP is the dissociation strongly reduced, pointing toward an entangled state similar to the crystal structure of yHsp90 with AMP-PNP.

In Supplementary Table 2, we compare the obtained values for the distances in between various amino acids in view of the yHsp90 crystal structure in the presence of the non-hydrolyzable ATP analogue AMP-PNP and the cochaperone p23/Sba1.[19] The distance between the N-terminal cysteine in the yHsp90 crystal structure is 7.1 nm and thus bigger than the measured values for HtpG (4.3 nm). This indicates that the N-terminal domain seems to be differently oriented than in the yHsp90 crystal. In our opinion, this can only be explained by some kind of N-terminal rotation compared to the yHsp90 crystal structure. The distance for the middle domain at position 341C is 2.4 nm in the yHsp90 crystal, and thus, HtpG is more extended or also rotated in the middle domain. The C-terminal cysteines in yHsp90 have a distance of around 4.7 nm, in good agreement with the measured values. Taken together, the C--terminal orientation seems to be similar in HtpG and yHsp90, whereas the M-domain and the N-domain are differently oriented in HtpG compared to the AMP-PNP-bound yHsp90. Within the uncertainty of the measurements, the HtpG structures based on small-angle X-ray scattering (see Supplementary Table 2) are also consistent with our measured values if a rotation of the N-terminal domains is assumed. For a more detailed discussion, see Supplementary Text.

What could be the advantage of the observed increased flexibility and only marginal control by nucleotides for yHsp90 compared to HtpG? First, a flexible protein can adapt to different types of substrate with greater ease than a rigid one. This might be important since the number of different proteins that have to be protected from aggregation upon heat shock is bigger for yHsp90 compared to that for HtpG.[20–22] Second, HtpG was recently shown to wrap around a substrate.[23] Such an "enclosing" of substrates could be much easier for the more flexible yHsp90. Third, more flexible chaperones (i.e., proteins with shallow energy barriers) can be much easier controlled by cochaperones. Since the different conformational states are separated by only shallow energy barriers, small binding energies are sufficient to significantly shift the conformational equilibrium. This might explain why no cochaperones for HtpG are known whereas a large number of these proteins are known for yHsp90. Additionally, it could explain why cochaperones with very little binding energies such as Aha1 or p23 (both have dissociation constants in the lower micromolar range[24,25]) are able to control the conformation of yHsp90.

In this context, what might be the advantage of the more pronounced C-terminal dynamics in yHsp90 compared to HtpG? Our data allow us to speculate that the additional C-terminal opening in yHsp90 effectively increases the accessible surface of the protein, providing more possibilities for client binding. Furthermore, it allows the substrate to enter from two sides of the inner part of the protein, which is thought to be the client binding region. Thus, C-terminal opening increases the modes of substrate binding and might allow processing of a greater variety of clients.

Finally, the anti-correlated movement in between the N-terminus and the C-terminus hinders yHsp90 from falling apart despite the high flexibility. This is very important because monomers are not functional *in vivo*.[13] Thus, this anti-correlation effectively increases the amount of dimer and, thus, the overall chaperoning efficiency in the cell.

We can only speculate on the remaining questions, namely, why did the obvious evolution from a nucleotide-regulated ordered mechanism toward a random fluctuating network of states takes place? Why the controlled mechanism of HtpG had to be replaced by the random fluctuation of yHsp90? As we already pointed out above, the number, as well as the size, of the proteins in the cell increased from bacteria to yeast. Therefore, a more effective chaperoning might be necessary. Another observation is that the role of Hsp90 in the cell seems to have changed from bacteria to yeast. Thus, *Escherichia coli* without the HtpG-encoding gene is still viable, but yeast does not survive without any functional Hsp90. Finally, a lot of the known yHsp90 substrates are involved in cell regulation and signal transduction. Thus, in eukaryotic cells, Hsp90 has a more important role in cellular processes, which might have caused an evolution toward a more sophisticated chaperone system.

In summary, we observe a clear change in protein mechanism between the prokaryotic HtpG and the eukaryotic yHsp90. yHsp90 has a higher N-terminal flexibility, a new C-terminal dynamics, and an anti-correlation between N- and C-terminal dynamics to increase its potential to bind various substrate proteins and, at the same time, stay in its functional dimeric form. Although we do not know which evolutionary pressure lead to this type of change in the protein mechanism, our findings show that noisy systems, which have smaller energetic differences in between their conformational states, can be favorable since they can adopt much better to changing tasks and show a greater functionality.

Materials and Methods

Cloning, expression, and protein purification

Cloning, expression, and purification were performed as described previously[11,26] and detailed in Supplementary Information.

Protein labeling and biotinylation

The protein was labeled by maleimide chemistry as described previously.[8,9] The labeling efficiency was checked by measuring the dye and protein concentration by UV/Vis absorption spectroscopy. The labeling efficiency was close to 100% (±15%). Biotinylation was performed as described previously.[8] For more detailed information, see Supplementary Information.

Bulk measurement of ATP binding

Fluorescence measurements were performed with a FP-6500 fluorometer (Jasco, Easton, MD, USA). The HtpG labeled at the cysteine at position 61 without C-terminal zipper was pre-incubated at 30 °C at a concentration of 1 μM in the cuvette. After 2 min of pre-incubation, 10 μM Atto647N-labeled ATP at γ position (Atto Tec, Siegen) was added to the protein. The sample was excited at 532 nm and the fluorescence was detected at 580 nm and 675 nm.

Bulk measurement of monomer exchange

HtpG was pre-incubated at a concentration of 500 nM for each monomer (50 nM, respectively, for the measurement shown in Supplementary Fig. 5) without or with 2 mM ADP/ATP/AMP-PNP at 30 °C for 15 min to reach equilibrium. Then, the two differently labeled monomers were mixed 1:1 with a final concentration of 250 nM (25 nM). The exchange was followed by measuring the fluorescence intensities of the donor (580 nm) and the acceptor (675 nm) after donor excitation (530 nm).

Single-molecule measurements

All single-molecule fluorescence measurements were performed in a custom-built prism-type total internal reflection fluorescence microscope equipped with three lasers [473 nm Cobolt Blues, 50 mW (Stockholm, Sweden); 532 nm Compass 215M, 75 mW (Coherent Inc., Santa Clara, CA, USA); and 635 nm LPM635-25C, 25 mW (Newport, Irvine, CA, USA)]. The excitation intensity was around 2 mW at the measurement chamber for all measurements. The setup is furthermore equipped with an Acusto Optical Filter (AOTFnC-Vis; AAOptics, Orsay Cedex, France), which was triggered by the camera switching on the laser light only when the camera was collecting light. For the two-color measurements, the sample was illuminated with the 532-nm laser. For the measurement of the N-terminal dynamics of HtpG, the sample was illuminated 200 ms every second in the case of inter-domain measurements and 200 ms with a 20-ms delay time in the case of intra-monomer measurements (to minimize photo degradation of the dye and to optimize the observation times). The measurements were analogous to those of Mickler *et al*.[8]

The C-terminal dynamics was recorded with 200 ms camera illumination and 20 ms delay with green-laser excitation (532 nm). The measurements of C-terminal movement were analogous to those of Ratzke *et al*.[9] For the three-color measurements, the sample was illuminated with the 473-nm laser with 200 ms illumination and 20 ms delay times. The detection and analysis are described in Supplementary Information.

Acknowledgements

We thank Judith Schiefer and Björn Hellenkamp for helpful discussions and Noland Holland for critical reading of the manuscript. Support by the Nanosystems Initiative Munich and the German Science Foundation to T.H. (Hu997/9-1 and SFB 863) and M.P.M. (SFB 638) is gratefully acknowledged. C.R. is supported by the Internationales Doktorandenkolleg "NanoBioTechnologie" program of the Elitenetzwerk Bayern.

Supplementary Data

Supplementary data to this article can be found online at http://dx.doi.org/10.1016/j.jmb.2012.07.026

References

1. Arsene, F., Tomoyasu, T. & Bukau, B. (2000). The heat shock response of *Escherichia coli*. *Int. J. Food Microbiol.* **55**, 3–9.
2. Mayer, M. P. (2010). Gymnastics of molecular chaperones. *Mol. Cell*, **39**, 321–331.
3. Wandinger, S. K., Richter, K. & Buchner, J. (2008). The Hsp90 chaperone machinery. *J. Biol. Chem.* **283**, 18473–18477.
4. Pearl, L. H., Prodromou, C. & Workman, P. (2008). The Hsp90 molecular chaperone: an open and shut case for treatment. *Biochem. J.* **410**, 439–453.
5. Krukenberg, K. A., Street, T. O., Lavery, L. A. & Agard, D. A. (2011). Conformational dynamics of the molecular chaperone Hsp90. *Q. Rev. Biophys.* **44**, 229–255.
6. Chen, B., Zhong, D. B. & Monteiro, A. (2006). Comparative genomics and evolution of the HSP90 family of genes across all kingdoms of organisms. *BMC Genomics*, **7**, 19.
7. Hessling, M., Richter, K. & Buchner, J. (2009). Dissection of the ATP-induced conformational cycle of the molecular chaperone Hsp90. *Nat. Struct. Mol. Biol.* **16**, 287–293.
8. Mickler, M., Hessling, M., Ratzke, C., Buchner, J. & Hugel, T. (2009). The large conformational changes of Hsp90 are only weakly coupled to ATP hydrolysis. *Nat. Struct. Mol. Biol.* **16**, 281–286.
9. Ratzke, C., Mickler, M., Hellenkamp, B., Buchner, J. & Hugel, T. (2010). Dynamics of heat shock protein 90 C-terminal dimerization is an important part of its conformational cycle. *Proc. Natl Acad. Sci. USA*, **107**, 16101–16106.
10. Shiau, A. K., Harris, S. F., Southworth, D. R. & Agard, D. A. (2006). Structural analysis of *E. coli* hsp90 reveals dramatic nucleotide-dependent conformational rearrangements. *Cell*, **127**, 329–340.
11. Graf, C., Stankiewicz, M., Kramer, G. & Mayer, M. P. (2009). Spatially and kinetically resolved changes in the conformational dynamics of the Hsp90 chaperone machine. *EMBO J.* **28**, 602–613.
12. Richter, K. & Buchner, J. (2006). Hsp90: twist and fold. *Cell*, **127**, 251–253.
13. Wayne, N. & Bolon, D. N. (2007). Dimerization of Hsp90 is required for *in vivo* function. Design and analysis of monomers and dimers.. *J. Biol. Chem.* **282**, 35386–35395.
14. Lakowicz, J. R. (2006). *Principles of Fluorescence Spectroscopy*, 3rd edit Springer, New York, NY.
15. Ratzke, C., Berkemeier, F. & Hugel, T. (2012). Hsp90's mechano-chemical cycle is dominated by thermal fluctuations. *Proc. Natl Acad. Sci. USA*, **109**, 161.
16. Krukenberg, K. A., Forster, F., Rice, L. M., Sali, A. & Agard, D. A. (2008). Multiple conformations of *E. coli* Hsp90 in solution: insights into the conformational dynamics of Hsp90. *Structure*, **16**, 755–765.
17. Clamme, J. P. & Deniz, A. A. (2005). Three-color single-molecule fluorescence resonance energy transfer. *ChemPhysChem*, **6**, 74–77.
18. Roy, R., Kozlov, A. G., Lohman, T. M. & Ha, T. (2009). SSB protein diffusion on single-stranded DNA stimulates RecA filament formation. *Nature*, **461**, 1092–1097.
19. Ali, M. M., Roe, S. M., Vaughan, C. K., Meyer, P., Panaretou, B., Piper, P. W. *et al.* (2006). Crystal structure of an Hsp90–nucleotide–p23/Sba1 closed chaperone complex. *Nature*, **440**, 1013–1017.
20. Blattner, F. R., Plunkett, G., III, Bloch, C. A., Perna, N. T., Burland, V., Riley, M. *et al.* (1997). The complete genome sequence of *Escherichia coli* K-12. *Science*, **277**, 1453–1462.
21. Mewes, H. W., Albermann, K., Bahr, M., Frishman, D., Gleissner, A., Hani, J. *et al.* (1997). Overview of the yeast genome. *Nature*, **387**, 7–65.
22. Netzer, W. J. & Hartl, F. U. (1997). Recombination of protein domains facilitated by co-translational folding in eukaryotes. *Nature*, **388**, 343–349.
23. Street, T. O., Lavery, L. A. & Agard, D. A. (2011). Substrate binding drives large-scale conformational changes in the Hsp90 molecular chaperone. *Mol. Cell*, **42**, 96–105.
24. Lotz, G. P., Lin, H., Harst, A. & Obermann, W. M. (2003). Aha1 binds to the middle domain of Hsp90, contributes to client protein activation, and stimulates the ATPase activity of the molecular chaperone. *J. Biol. Chem.* **278**, 17228–17235.
25. Richter, K., Walter, S. & Buchner, J. (2004). The co-chaperone Sba1 connects the ATPase reaction of Hsp90 to the progression of the chaperone cycle. *J. Mol. Biol.* **342**, 1403–1413.
26. Richter, K., Muschler, P., Hainzl, O. & Buchner, J. (2001). Coordinated ATP hydrolysis by the Hsp90 dimer. *J. Biol. Chem.* **276**, 33689–33696.